Systematic study of doping dependence on linear magnetoresistance in p-PbTe

J. M. Schneider, M. L. Peres, S. Wiedmann, U. Zeitler, V. A. Chitta, E. Abramof, P. H. O. Rappl, S. de Castro, D. A. W. Soares, U. A. Mengui, and N. F. Oliveira Jr.

Articles you may be interested in

Room temperature persistent photoconductivity in p-PbTe and p-PbTe:BaF2
Appl. Phys. Lett. **105**, 162105 (2014); 10.1063/1.4899140

Fermi level pinning in Fe-doped PbTe under pressure
Appl. Phys. Lett. **105**, 022101 (2014); 10.1063/1.4890381

Thermoelectric properties of Bi-doped PbTe composites
J. Appl. Phys. **109**, 103709 (2011); 10.1063/1.3586240

Electrical properties of PbTe doped with BaF 2
J. Appl. Phys. **105**, 043709 (2009); 10.1063/1.3082043

Temperature dependence of the Seebeck coefficient and the potential barrier scattering of n-type PbTe films
prepared on heated glass substrates by rf sputtering
J. Appl. Phys. **92**, 5331 (2002); 10.1063/1.1512964

Systematic study of doping dependence on linear magnetoresistance in *p*-PbTe

J. M. Schneider,[1] M. L. Peres,[2,a)] S. Wiedmann,[3] U. Zeitler,[3] V. A. Chitta,[1] E. Abramof,[4] P. H. O. Rappl,[4] S. de Castro,[2] D. A. W. Soares,[2] U. A. Mengui,[4] and N. F. Oliveira, Jr.[1]

[1]*Instituto de Física, Universidade de São Paulo, São Paulo, PB 66318, São Paulo CEP 05315-970, Brazil*
[2]*Departamento de Física e Química, Universidade Federal de Itajubá, Itajubá, PB 50, Minas Gerais CEP 37500-903, Brazil*
[3]*Radboud University Nijmegen, Institute for Molecules and Materials, High Field Magnet Laboratory, Toernooiveld 7, 6525 ED Nijmegen, The Netherlands*
[4]*Laboratório Associado de Sensores e Materiais, Instituto Nacional de Pesquisas Espaciais, São José dos Campos, PB 515, São Paulo CEP 12201-970, Brazil*

We report on a large linear magnetoresistance effect observed in doped *p*-PbTe films. While undoped *p*-PbTe reveals a sublinear magnetoresistance, *p*-PbTe films doped with BaF_2 exhibit a transition to a nearly perfect linear magnetoresistance behaviour that is persistent up to 30 T. The linear magnetoresistance slope $\Delta R/\Delta B$ is to a good approximation, independent of temperature. This is in agreement with the theory of Quantum Linear Magnetoresistance. We also performed magnetoresistance simulations using a classical model of linear magnetoresistance. We found that this model fails to explain the experimental data. A systematic study of the doping dependence reveals that the linear magnetoresistance response has a maximum for small BaF_2 doping levels and diminishes rapidly for increasing doping levels. Exploiting the huge impact of doping on the linear magnetoresistance signal could lead to new classes of devices with giant magnetoresistance behavior. © 2014 AIP Publishing LLC. [http://dx.doi.org/10.1063/1.4900486]

The rather unusual linear response of the sample resistance as a function of the magnetic field was already discovered in the late 1920s in bismuth and polycrystalline metals.[1] While this effect has been forgotten for a long time, its (re-)discovery in silver chalcogenides[2] attracted a lot of interest due to possible applications in magnetosensor devices.[3] Since then, linear magnetoresistance (LMR) has been reported in numerous materials such as InAs films,[4] YPdBi Heusler topological insulators,[5] InSb,[6] silicon,[7,8] epitaxial graphene,[9] $Ba(FeAs)_2$,[10] Bi_2Se_3,[11,12] and Bi_2Se_3/Bi_2Te_3 heterostructure.[13]

The origin of LMR in these materials is subject of often controversial discussions. For materials with closed Fermi surfaces, two theories are at play: Abrikosov's Quantum LMR (QLMR) model[14,15] and the Parish-Littlewood (PL) model.[16,17] According to Abrikosov, LMR is observed in the quantum limit, when all charge carriers occupy the lowest Landau level. In the PL model, LMR is a classical effect resulting from microscopically distorted current paths in highly disordered samples. Voltage simulations show that the LMR is provided internally by the Hall effect, which is in agreement with results obtained from polycrystalline Al plates.[18] For *p*-PbTe based structures, the LMR phenomena has not been reported so far.

PbTe is a well-known high mobility, narrow-gap IV-VI semiconductor, with Fermi surfaces consisting of four equivalent ellipsoids at the *L* point of the Brillouin zone.[19] Its extraordinary physical properties make PbTe a base material of infrared optoelectronics.[20] In addition, the physics is further enriched by the large value of the Landé *g* factor and the small effective mass, both of which display considerable anisotropy. Such properties make PbTe an interesting material for possible applications in spintronics. Recently, PbTe was suggested for use as a spin filter[21] since the large value of the Landé *g* factor should permit such devices to operate at low magnetic fields.

In this work, we report on a large LMR effect in *p*-PbTe films doped with BaF_2. Moreover, we present a systematic study of how different doping levels affect the magnitude of the LMR signal. We also show that while undoped non-stoichiometric PbTe reveals a sublinear magnetoresistance (MR), *p*-PbTe doped with BaF_2 exhibits a nearly perfect, non-saturating LMR signal. The largest LMR response is observed in low doping samples, with BaF_2 doping levels of 0.02%. For increasing doping levels (0.04%–1%), the LMR signal diminishes rapidly. For all samples, the LMR slopes $\Delta R/\Delta B$ are to a good degree of accuracy independent of temperature. This is consistent with the theory of QLMR. The scattering center concentration extracted from the QLMR model increases with increasing doping levels, which ultimately leads to a decrease of the hole mobility. Finally, we compare the LMR data with the classical PL model. Simulations of the LMR slopes $\Delta R/\Delta B(T)$ using the PL model reveal a strong temperature dependence, which is inconsistent with the data investigated in this work. The large linear magnetoresistance signal observed in the *p*-type PbTe samples could lead to new classes of devices with huge linear magnetoresistance behavior.

For the electrical transport measurements, millimeter-size, about $d = 3.4\,\mu m$ thick pieces of non-stoichiometric *p*-PbTe with BaF_2 doping levels between 0.02% and 1% were contacted in approximate Van der Pauw geometry by soldering Au wires with In pellets. A comprehensive description of

---
a)Author to whom correspondence should be addressed. Electronic mail: marcelos@unifei.edu.br

the sample growth procedure together with a detailed electrical characterization is given in Ref. 22. The main measurements were performed in a 15 T He-cooled superconducting magnet, using an ac current of 50 μA at 10.7 Hz and conventional phase sensitive detection. The high field measurements were performed in a 33 T resistive magnet.

The magnetic field was applied along the [111] direction of PbTe. In Figure 1, we plot an overview of the longitudinal MR normalized to its zero field value R_0 of both undoped (a) and doped p-PbTe (b)–(d) for selected temperatures in the range $T = 4.2$–200 K ($B = 0$–15 T). The Hall component in the MR signal due to the imperfect geometry of the contacts was subtracted by measuring both at positive and negative polarization of the magnetic field. It is possible to observe that all samples reveal a strong MR decrease for increasing temperatures. Quantum oscillations are not observed even at large values of magnetic fields, which is probably linked to the large MR background signal. In Figure 1(a), one observes that undoped p-PbTe exhibits a sublinear MR, and at $B = 15$ T and $T = 4.2$ K, the MR increase is about 600%. In Figure 1(b), the MR of p-PbTe with the lowest BaF$_2$ doping level, 0.02%, is depicted. At $B_0 \sim 0.4$ T, a transition from a classical, parabolic MR to a nearly perfect LMR is observed (Figure 1(b) inset) and at $B = 15$ T and $T = 4.2$ K the LMR is ~6000%, which is about 10 times larger than in undoped p-PbTe. This is one of the largest LMR values reported in literature so far.[8,17] At $T = 200$ K, the LMR increase is still about 200%. Figures 1(c) and 1(d) show the MR for samples with doping levels of 0.04% and 0.6%, respectively. The LMR resembles the 0.02% data; however, the signals are significantly smaller, with increases of roughly 2000% and 250%, respectively.

The high field measurements are presented in Figure 2. Figure 2(a) shows that the LMR is non-saturating up to $B = 30$ T, remarkably revealing that the LMR effect is
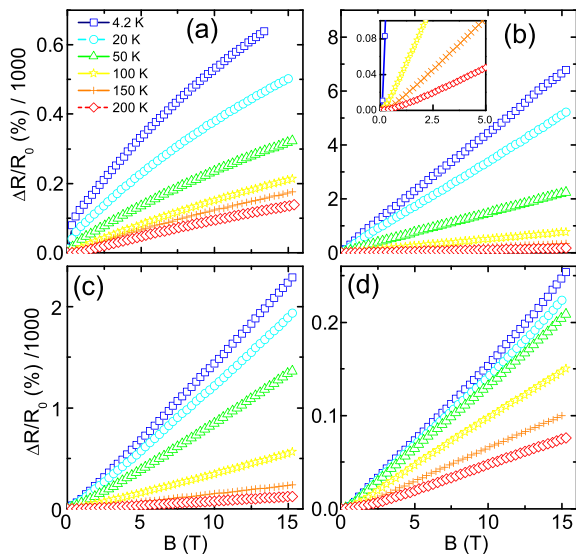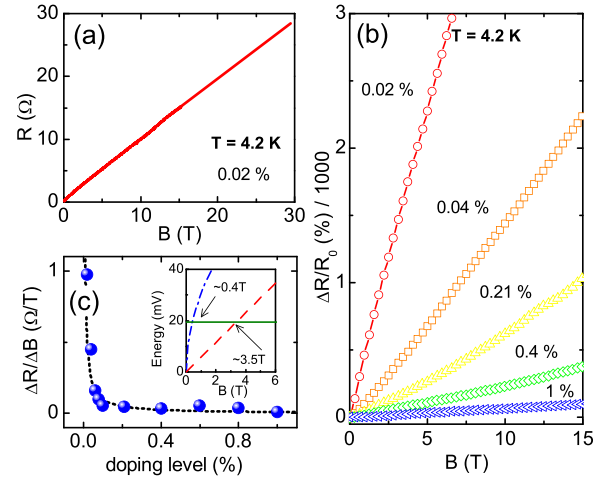

FIG. 2. (a) LMR for a sample with 0.02% doping. The curve is non-saturating up to $B = 30$ T. (b) $\Delta R/R_0$ measured at $T = 4.2$ K for samples with different BaF$_2$ doping levels between 0.02% and 1%, revealing the strong effect of the doping over the maximum LMR amplitude. (c) LMR slope $\Delta R/\Delta B$ measured at $T = 4.2$ K as a function of the doping levels. While the slope for the 0.02% sample is about 1 Ω/T, a rapid decrease to ~50 mΩ/T takes place when increasing the doping concentration to 0.1%. Inset: The solid line represents the Fermi energy with the cyclotron energy (dashed line) and the energy for materials with linear band dispersion (dashed-dotted line). The arrows indicate the interception points with the Fermi energy.

persistent in a wide range of magnetic field values. The strong suppression of the LMR signal is shown in more detail in Figure 2(b), where we plot $\Delta R/R_0$ measured at $T = 4.2$ K for samples with different BaF$_2$ doping levels between 0.02% and 1%. Figure 2(c) shows the LMR slope $\Delta R/\Delta B$ measured at $T = 4.2$ K as a function of the doping levels. The dashed line is a guide for the eye. While the slope for the 0.02% sample is about 1 Ω/T, a rapid decrease to ~50 mΩ/T takes place when increasing the doping concentration to 0.1%. For larger doping levels, the slope remains almost unchanged. We now compare the data to the predictions of the theoretical models for LMR, i.e., Abrikosov's QLMR model and the classical PL model. According to Abrikosov, LMR can occurs in the quantum limit when all charge carriers occupy the lowest Landau level[14,15] and the longitudinal component of the resistivity is then given by $\rho_{xx} = N_i B/\pi n^2 e$, where n is the density of charge carriers and N_i is the concentration of scattering centers. ρ_{xx} has no direct temperature dependence; however, $n(T)$ can introduce a temperature effect. The linear behavior arises from scattering of electrons between quantized orbits parallel to the magnetic field. Hence, the decrease of the radius of the orbits with increasing field decreases the collision probability, leading to a decrease of the conductivity.

Measurements of the charge carrier concentration as a function of the temperature show that in the samples studied in this work n is strictly independent on temperature, i.e., no charge carrier freeze out takes place (Figure 2 in Ref. 22). In Figure 3(a), we plot the LMR slopes $\Delta R/\Delta B$ for selected doping levels (0.02%, 0.04%, 0.06%, and 0.8%) as a function of temperature ($T = 4.2$–200 K). The slopes are to a good approximation independent on temperature (dotted lines), which is in accordance with the predictions of the QLMR-model, with n being independent of temperature.
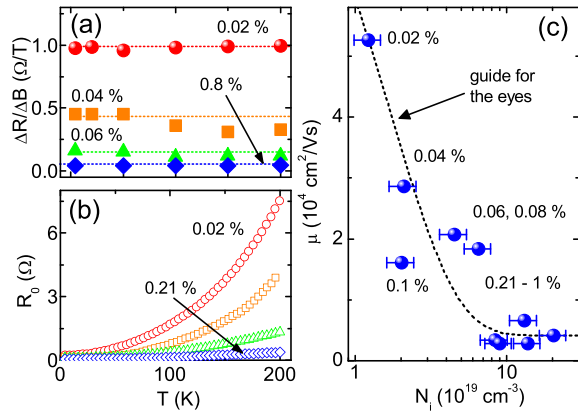

FIG. 1. (a) Undoped p-PbTe sample exhibits a sublinear MR and at $B = 15$ T and $T = 4.2$ K the MR increase is about 600%. (b) MR for the lowest BaF$_2$ doping level, 0.02%. A transition from a classical, parabolic MR, to a nearly perfect LMR, as can be observed in the inset, and at $B = 15$ T and $T = 4.2$ K the LMR is ~6000%. (c) MR for sample with doping level of 0.04% and (d) with doping level of 0.6%. In both figures, (c) and (d), the LMR resembles the 0.02% data; however, the signals are significantly smaller.

FIG. 3. (a) LMR slopes $\Delta R/\Delta B$ for selected doping levels (0.02%, 0.04%, 0.06%, and 0.8%) as a function of temperature ($T = 4.2$–200 K). The slopes are to a good approximation independent on temperature (dotted lines). (b) Zero field resistance $R_0(T)$, which is plotted for doping levels of 0.02%, 0.04%, 0.08%, and 0.21%, revealing a metallic behavior. (c) Mobilities at $T \sim 10$ K of each sample as a function of the scattering center concentration N_i.

The temperature dependence of the LMR data shown in Figure 1 comes solely from the temperature dependence of the zero field resistance $R_0(T)$, which is plotted in Figure 3(b) for doping levels of 0.02%, 0.04%, 0.08%, and 0.21%, revealing a metallic behavior.

Hence, for $B > B_0$, with B_0 being the onset magnetic field of LMR, the full magnetic field and temperature dependence of the resistivity is therefore given by $\rho_{xx}(B,T) = \rho_{xx}(T) + N_i B/\pi n^2 e$. Knowing the charge carrier concentrations of each sample, we can extract their scattering center concentration from the LMR slope $\Delta \rho_{xx}/\Delta B$. For the sample with the lowest doping level (0.02%), we obtain $N_i \approx 1.2 \times 10^{19} cm^{-3}$. For high doping levels (0.8%–1%), the scattering center concentration is about 10 times larger. In Fig. 3(c), we plot the 10 K mobilities of each sample (see Table I in Ref. 22) as a function of the scattering center concentration N_i. The error bars of the N_i values were estimated from small uncertainties in the LMR slopes and the conversion of the resistance values to resistivity values. The dashed line is a guide for the eye. The mobility has its largest values for low scattering concentrations and diminishes for increasing values of N_i, clearly demonstrating the mobility reducing effect of scattering.

In materials with parabolic band dispersion, the quantum limit is reached when $\hbar \omega_c > E_F$, with E_F being the Fermi energy and $\omega_c = eB/m^*$ is the cyclotron frequency. The

values of E_F are about 10 and 55 meV for the samples with doping levels 0.02% and 1%, respectively.[23] With $m^* \approx 0.02 m_0$,[19] the theoretical onset magnetic fields of LMR varies between $B_0 \approx 3.5 T$(lowest charge carrier concentration) and ≈ 20 T (highest concentration). The inset in Figure 2(c) shows the calculated Fermi energy for sample with doping level of 0.02% (solid line) and the cyclotron energy (dashed line). The arrow indicates the interception point at ~ 3.5 T. Experimentally, however, the onset magnetic field values are $B_0 < 2$ T for all samples according to Figures 1 and 2, regardless of the charge carrier concentration. This discrepancy between the experimental values and the theoretical prediction was also observed in the narrow-gap semiconductors Ag_2Te and InSb.[2,6] Abrikosov proposed two mechanisms, which can lead to smaller magnetic field values of the quantum limit to be reached: First, real samples contain inhomogeneities, which lead to regions of both large and small charge carrier concentrations. In regions with small charge carrier concentrations, i.e., small values of E_F, the extreme quantum situation takes place, leading to smaller onset magnetic field values of LMR.[14] Second, disorder in the sample can trigger a phase transition from a narrow-gap semiconductor to a gapless semiconductor with quasi-linear bandstructure.[24] In materials with linear band dispersion, the quantum limit is reached when $E_F = v_F \sqrt{2e\hbar B}$ (dashed-dotted line, Figure 2(c) inset) with v_F being the Fermi velocity. Ultimately, the linear band dispersion leads to considerably smaller onset magnetic fields of LMR[25] (see arrows in the inset). In PbTe, due to its small bandgap of $E_F = 190$ meV ($T = 0$ K),[19] the second effect is likely to happen. However, a direct observation of inhomogeneities induced changes of the band structure is still missing to date.

In order to obtain qualitative information about the disorder effect of BaF_2 doping on PbTe films, we performed scanning electron microscopy on the samples. Figure 4(a) reveals a clean image of an undoped PbTe sample. Figure 4(b) presents an image of a PbTe:BaF_2 film with doping content of 0.02%. A drastic modification of the image is observed, which is mainly due to inhomogeneities (dark dots). Hence, even for a small BaF_2 doping the disorder effect is considerable.

Sample inhomogeneities also play a crucial role in the second theoretical model of LMR, the PL model.[16,17] In the PL model, a strongly inhomogeneous conductor is modeled by discretization into a random resistor network. The PL model has no analytic solution. Simulations of the MR,
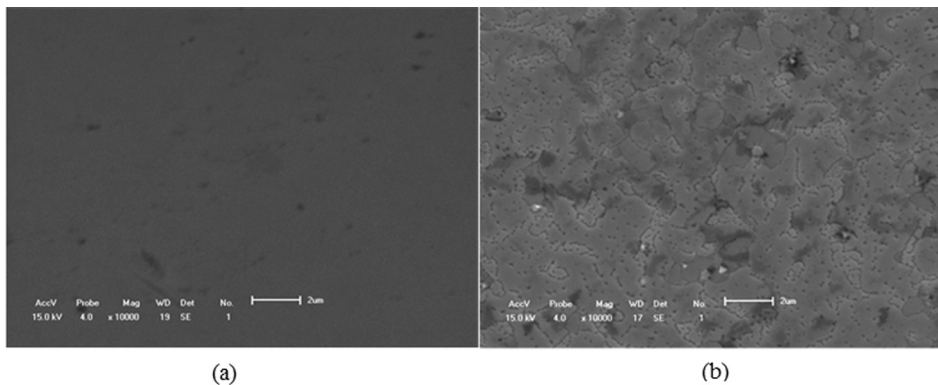

FIG. 4. Scanning electron microscopy images of a p-PbTe film without (a) and with 0.02% BaF_2 doping (b). The surface roughness and the dark dots show the introduction of inhomogeneities by doping.
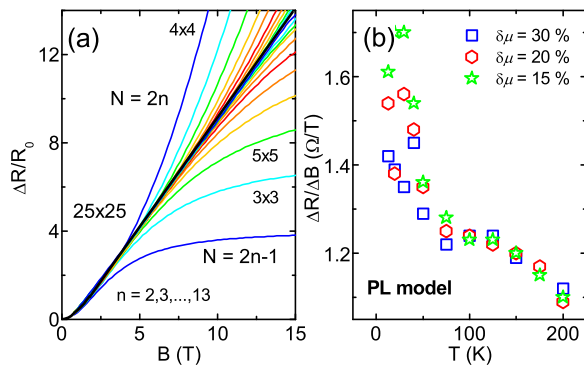
FIG. 5. (a) Simulated MR of $N \times N$ uniform networks with $N = 3$, 4,…, 25 ($R = 1\ \Omega$, $\mu = 1\ \text{m}^2/\text{V s}$). For large values of N ($N = 25$ for the parameters of R and μ used here), the curves collapse onto a straight line. (b) Simulated LMR slope $\Delta R/\Delta B$ for temperatures in the range $T = 4.2$–200 K. Unlike the experimental data, $\Delta R/\Delta B$ decreases by about 40% in the simulated temperature range.

however, show that $\Delta R/R_0 \propto \langle \mu \rangle$ for $\delta\mu/\langle\mu\rangle < 1$ with $\langle\mu\rangle$ being the average mobility and $\delta\mu$ representing the mobility fluctuations.[16] To better understand how the interplay between the average mobility, mobility fluctuations, and resistance fluctuations in influences the MR signal, we implemented numerical calculations based on the PL model. We used a two-dimensional square lattice constructed of interconnected four-terminal resistors, with an external magnetic field applied perpendicular to the network. Figure 5(a) shows the simulated MR of $N \times N$ uniform networks with $N = 3$, 4,…, 25 ($R = 1\ \Omega$, $\mu = 1\ \text{m}^2/\text{V s}$). The fact that networks with even N exhibit a non-saturating MR, whereas networks with odd N exhibit saturation, shows that our simulations are correct.[16] For large values of N ($N = 25$ for the parameters of R and μ used here), the curves collapse onto a straight line. Sample inhomogeneities are modeled by incorporating Gaussian distributed mobility fluctuations. In the following we used 25×25 networks, averaged over five random network configurations. As parameters we used the experimental values for the resistances and mobilities including $\delta\mu = 15 - 20$ mobility fluctuations. For $\delta\mu < 15\%$ the simulations reveal a non-linear, saturating MR, due to size effects of the network. Fig. 5(b) shows the simulated LMR slope $\Delta R/\Delta B$ for selected temperatures in the range $T = 4.2$–200 K. Unlike the experimental data, $\Delta R/\Delta B$ decreases by about 40% in the simulated temperature range, with $\Delta R/\Delta B(T)$ having an almost linear temperature dependence.

The fact that the observed LMR in samples investigated in this work is not a classical effect is confirmed by estimations of the Hall voltage variations δn. According to Ref. 26, $\langle \delta n \rangle / n \propto LMR/R_{xy}$ in polycrystalline samples. For the sample with doping level of 0.02%, the LMR signal at 10 T is 10 Ω. $R_{xy} = B/(ned) \approx 40\ \Omega$, so that δn is expected to be ≈ 25, which is nearly two orders of magnitude larger than the measured δn extracted from Hall measurements on different parts of the sample. Even though the PL model might explain the occurrence of LMR in materials such as $Fe_{1-x}Co_xSb_2$ single crystals[27] and $InAs_{1-x}N_x$,[28] it fails to explain the data in case of the narrow-gap semiconductor PbTe.

Very recently, the formation of a p-type layer in the region adjacent to the BaF_2 substrate due to the defects caused by dislocations has been found in n-type PbTe

epilayers.[29] Owing to a two-channel conduction, a positive magneto-resistance has been observed. However, this scenario can also be ruled out for the samples studied here since we did not find any experimental evidence for a second channel in our p-type PbTe films.

In conclusion, we showed that p-PbTe doped with BaF_2 reveals a large LMR signal. The LMR slopes $\Delta R/\Delta B$ of all the samples are to a good degree of accuracy independent of temperature, which is in agreement with the QLMR model. MR simulations using the PL model fail to explain the data. Moreover, we showed that the LMR response depends strongly on the doping level, i.e., increasing doping levels lead to a decrease in magnitude of LMR. The strong impact of especially low doping levels on the LMR response could be exploited for tailoring new classes of devices with large LMR behavior.

[1]P. Kapitza, Proc. R. Soc. London, Ser. A **123**, 292 (1929).
[2]R. Xu, A. Husmann, T. F. Rosenbaum, M. L. Saboungi, J. E. Enderby, and P. B. Littlewood, Nature **390**, 57 (1997).
[3]J. Heremans, J. Phys. D: Appl. Phys. **26**, 1149 (1993).
[4]N. V. Kozlova, N. Mori, O. Makarovsky, L. Eaves, Q. D. Zhuang, A. Krier, and A. Patanè, Nat. Commun. **3**, 1097 (2012).
[5]W. Wang, Y. Du, G. Xu, X. Zhang, E. Liu, Z. Liu, Y. Shi, J. Chen, G. Wu, and Xi.-X. Zhang, Sci. Rep. **3**, 2181 (2013).
[6]J. Hu and T. F. Rosenbaum, Nat. Mater. **7**, 697 (2008).
[7]M. P. Delmo, S. Yamamoto, S. Kasai, T. Ono, and K. Kobayashi, Nature **457**, 1112 (2009).
[8]N. A. Porter and C. H. Marrows, Sci. Rep. **2**, 565 (2012).
[9]A. L. Friedman, J. L. Tedesco, P. M. Campbell, J. C. Culbertson, E. Aifer, F. K. Perkins, R. L. Myers-Ward, J. K. Hite, C. R. Eddy, Jr., G. G. Jernigan, and D. K. Gaskill, Nano Lett. **10**, 3962 (2010).
[10]K. K. Huynh, Y. Tanabe, and K. Tanigaki, Phys. Rev. Lett. **106**, 217004 (2011).
[11]H. Tang, D. Liang, R. L. J. Qiu, and X. P. A. Gao, ACS Nano **5**, 7510 (2011).
[12]H. He *et al.*, Appl. Phys. Lett. **100**, 032105 (2012).
[13]Y. Zhao, C.-Zu. Chang, Y. Jiang, A. Da Silva, Y. Sun, H. Wang, Y. Xing, Y. Wang, K. He, X. Ma, Qi.-K. Xue, and J. Wang, Sci. Rep. **3**, 3060 (2013).
[14]A. A. Abrikosov, Phys. Rev. B **58**, 2788 (1998).
[15]A. A. Abrikosov, Europhys. Lett. **49**, 789 (2000).
[16]M. M. Parish and P. B. Littlewood, Nature **426**, 162 (2003).
[17]J. Hu, M. M. Parish, and T. F. Rosenbaum, Phys. Rev. B **75**, 214203 (2007).
[18]G. J. C. L. Bruls, J. Bass, A. P. van Gelder, H. van Kempen, and P. Wyder, Phys. Rev. B **32**, 1927 (1985).
[19]D. Khokhlov, *Lead Chalcogenides* (Tayler & Francis Books, Inc., 2003).
[20]R. E. Harris, Laser Focus/Electro-Opt. **19**, 87 (1983).
[21]G. Grabecki, J. Appl. Phys. **101**, 081722 (2007).
[22]U. A. Mengui, E. Abramof, P. H. O. Rappl, B. Díaz, H. Closs, J. R. Senna, and A. Y. Ueta, J. Appl. Phys. **105**, 043709 (2009).
[23]J. R. Burke, B. Houston, and H. T. Savage, Phys. Rev. B **2**, 1977 (1970).
[24]A. A. Abrikosov, J. Low Temp. Phys. **8**, 315 (1972).
[25]A. A. Abrikosov, J. Phys. A: Math. Gen. **36**, 9119 (2003).
[26]A. M. Chang and D. C. Tsui, Solid State Commun. **56**, 153 (1985).
[27]R. Hu, K. J. Thomas, Y. Lee, T. Vogt, E. S. Choi, V. F. Mitrović, R. P. Hermann, F. Grandjean, P. C. Canfield, J. W. Kim, A. I. Goldman, and C. Petrovic, Phys. Rev. B **77**, 085212 (2008).
[28]A. Patanè, W. H. M. Feu, O. Makarovsky, O. Drachenko, L. Eaves, A. Krier, Q. D. Zhuang, M. Helm, M. Goiran, and G. Hill, Phys. Rev. B **80**, 115207 (2009).
[29]K. A. Kolwas, G. Grabecki, S. Trushkin, J. Wróbel, M. Aleszkiewicz, Ł. Cywiński, T. Dietl, G. Springholz, and G. Bauer, Phys. Status Solidi B **250**, 37 (2013).